In-Flight Calibration of an Interplanetary Navigation Instrument

THOMAS C. DUXBURY* AND HIROSHI OHTAKAY†
Jet Propulsion Laboratory, Pasadena, Calif.

This paper presents the results of an analytical investigation which demonstrates the feasibility of geometrically calibrating a navigation instrument during interplanetary flight to arc-sec accuracy. The instrument, similar to a television camera, would view selected natural satellites and reference stars simultaneously for navigating to the outer planets. An 11 × 11 reseau grid, etched onto the target raster of a vidicon tube, would be used to remove electromagnetic distortion from the satellite and reference star data to less than 1.2 arc-sec (1σ) in each and every data frame, independent of reseau data from any other data frame. Taking advantage of expected optical distortion stability, a total of fifty star images obtained from many data frames would be used to determine optical distortion to less than 4.3 arc-sec (1σ). Therefore, the use of the reseau grid and star images could enable the navigation measurements to be geometrically calibrated to an accuracy of 5 arc-sec (1σ).

Introduction

LIMITATIONS of Earth-based radio navigation capabilities for proposed multiple-outer planet missions[1] motivated the development of a spacecraft-based navigation data source. Spacecraft-based data would be used to augment Earth-based radio tracking data during the approach to a target planet so as to obtain an accurate estimate of the spacecraft trajectory relative to the target planet. Increased approach trajectory accuracy would permit a more accurate control of the flyby trajectory, which would significantly decrease the amount of spacecraft weight needed for trajectory correction purposes and increase the probability of successfully performing the multiple-outer planet missions.

The most useful information that the spacecraft-based data could supply to the navigation process would be the celestially referenced direction to the center-of-mass of the outer planet-satellite system.[2] An instrument[3] capable of producing this information is a television camera designed to view selected natural satellites and reference stars simultaneously during planet approach. Star data would be used to celestially reference the satellite directions, and satellite data would be used to determine the locations of the center-of-mass of the planet-satellite system.

Since the positions of the outer planet natural satellites are not known to many thousands of km, the orbital elements of these natural satellites would have to be estimated together with the spacecraft trajectory in the navigation process. Sufficient satellite/star data would be taken during planet approach to allow the determination of the natural satellite/spacecraft trajectory parameters to an accuracy limited only by the instrument measurement accuracy.

The instrument, producing optical measurements while many millions of kilometers from the target planet, is required to produce the direction information to an accuracy of 5 arc-sec (1σ) to obtain trajectory estimation accuracies of a few hundred kilometers.[4] The trajectory correction capability required for a variety of multiple-outer planet missions is shown in Fig. 1 as a function of optical measurement accuracy.[4] The missions considered were the Jupiter-Saturn-Uranus-Neptune missions with inner ring (GTA) and outer ring (GTB) passages at Saturn, the 1978 and 1979 Jupiter-Uranus-Neptune missions, and the 1977 Jupiter-Saturn-Pluto mission. Accuracies of 5 arc-sec (1σ) are possible with the use of calibration markings (reseau grid) on the face of the image tube of the instrument and by imaging star clusters. This article discusses the error sources associated with the instrument, the modeling of these errors, and the use of a reseau grid and star clusters to remove these errors from the flight data. The expected calibration accuracy together with the sensitivity of this accuracy to error parameters and the number of points in the reseau grid and stars used for calibration are also discussed.

Received Sept. 9, 1970; revision received July 15, 1971. This paper presents the results of one phase of research carried out at Jet Propulsion Laboratory, California Institute of Technology, under Contract 7-100, sponsored by the NASA.

* Task Leader, Mission Analysis Division. Member of AIAA.
† Senior Engineer, Guidance and Control Division.

Instrument Description

The proposed instrument, having a 3 × 3-deg field-of-view (FOV), would image selected natural satellites and reference stars simultaneously on an active target raster of a vidicon tube. The target raster would be scanned at 1000 lines with 1000 picture elements (pixels) per scan line giving an angular resolution of ±5 arc-sec per pixel. The instrument would be mounted on a two-axis gimbaled platform allowing a large total viewing capability.

The instrument would provide information of electromagnetic deflection voltages controlling the location at which the electron-scanning beam samples the target raster and also information of image intensity of the pixel being sampled. The deflection voltages would give a measure of the pixel location being sampled while the measure of pixel intensity would aid in identifying the image. The measured locations of images combined with instrument transfer characteristics would be used to determine the directions of objects. Geometric distortion of the image relationships occurring in the electron beam scanning circuitry (electromagnetic distortion) and in the telescope of the instrument (optical distortion) corrupts the direction measurement. Errors in instrument parameters (e.g., focal length) also corrupt the measured direction.

Sources of electromagnetic distortion include:[5] 1) nonuniform magnetic deflection field; 2) fringe field outside the deflection region of a vidicon tube; 3) interaction between the focusing and deflection fields; 4) nonuniform electric deceleration field; 5) electromagnetic bias shifts; 6) a common rotation of the scan deflection fields with respect to the target raster; and 7) a nonorthogonality of the scan line and pixel deflection fields.

The effect of the target planet magnetic field can be neglected since the spacecraft would be about 100 to 1000 planet radii away when the navigation data would be taken. Sources 1 and 2 cause symmetric radial distortions about the electromagnetic null point. Source 5 causes a shift (null-offset) of the null point. Error sources 5, 6, and 7 are illustrated in Fig. 2 where $\mathbf{x}_n$ represents the offset of the electromagnetic null point from the center of the target raster, ξ_1 represents

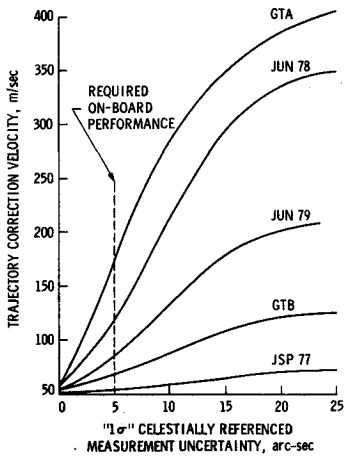

Fig. 1 Navigation system performance as a function of onboard instrument measurement uncertainty.

the common rotation of the deflection fields, and ξ_2 represents the nonorthogonality between the deflection fields. The symbols X_1 and X_2 define an orthogonal, absolute reference system determined from pre-launch measurement and ξ_1 and ξ_2 would be small angles.

Sources of optical distortion include[5]: 1) imperfect design and/or development of the telescope lens; 2) misalignment (nonorthogonality) of the lens optical axis with the target raster; and 3) decentering of the lens optical axis with respect to the center of the target raster.

Source 1 causes symmetric radial distortions about the optical principal point (intersection of the optical axis with the target raster). Source 2 causes asymmetric radial and tangential distortion about the principal point. Also, sources 2 and 3 cause a null-offset of the principal point from the center of the target raster.

An error in the value of focal length used to describe the instrument transfer function causes a symmetric radial distortion about the principal point. Errors in the values of pointing direction used to describe the instrument transfer function have a similar effect as errors in the values used for the location of the principal point on the target raster.

Instrument Measurement Model

The instrument will provide measurements of scanning beam deflection voltages which can be related to a physical location on the target raster. An arbitrary coordinate system in which to define image location measurements is an $x_1x_2x_3$ system (Fig. 3), where x_1 is in the plane of the target raster and in the direction of increasing pixel, x_2 is in the plane of the target raster and in the direction of increasing scan line, and x_3 is normal to x_1x_2. The origin of $x_1x_2x_3$ is chosen to be at the measured center (from flight data) of the target raster which is the nominal location of the electromagnetic null and also the optical principal point. The coordinate axis x_3 is in the direction of the nominal optical axis (outward from the instrument).

A general expression for the measured image location of an object (i.e., star or satellite) in front of the optics, based on the colinearity equation of photogrammetry,[6] is given by

$$\mathbf{x}_m = (f/w)C(I - E)M\mathbf{t} + \mathbf{x}_{op} + \mathbf{x}_{em} + \mathbf{n} \qquad (1)$$

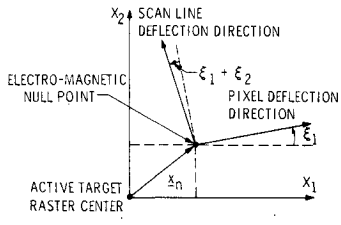

Fig. 2 Electromagnetic errors.

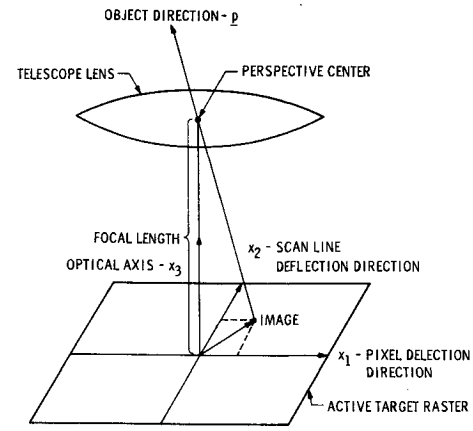

Fig. 3 Image geometry.

and a general expression for the measured image location of an object (reseau) on the target raster is given by

$$\mathbf{x}_m = \mathbf{x}_a + \mathbf{x}_{em} + \mathbf{n} \qquad (2)$$

where the lower case boldface letters denote 2×1 vectors, unless otherwise mentioned, the upper case letters designate matrices and, f is the effective optical focal length of the instrument; M is the transformation matrix from an inertial reference system to a nominal instrument reference system calculated from telemetered measurements (which contain errors) of instrument pointing direction;

$$C = \begin{bmatrix} 1 & 0 & 0 \\ 0 & 1 & 0 \end{bmatrix}$$

$\mathbf{t}$ is the spacecraft-centered inertial unit direction to an object; w is the third component of the 3×1 unit vector; $\mathbf{p} = M\mathbf{t}$, $\mathbf{n}$ is measurement noise vector due to pixel and scan line resolution; $\mathbf{x}_a$ is the absolute physical location of a reseau on the target raster determined precisely in X_1X_2 from prelaunch measurements.

The term $(I - E)$ is a rotation matrix that defines the deviation of the actual instrument orientation from the measured orientation. For small deviation angles ϵ_1, ϵ_2, and ϵ_3, $(I - E)$ is approximated by

$$(I - E) = \begin{bmatrix} 1 & \epsilon_3 & -\epsilon_2 \\ -\epsilon_3 & 1 & \epsilon_1 \\ \epsilon_2 & -\epsilon_1 & 1 \end{bmatrix} \qquad (3)$$

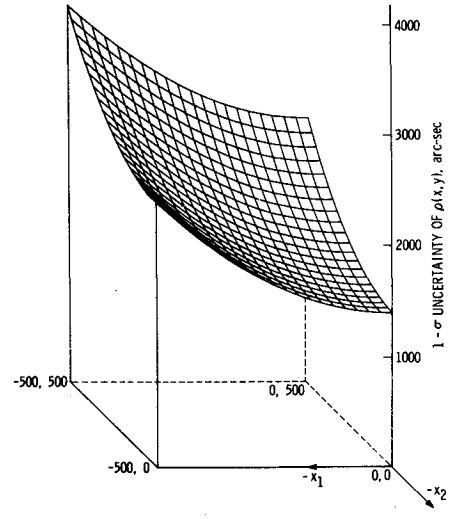

Fig. 4 Electromagnetic a priori uncertainty.

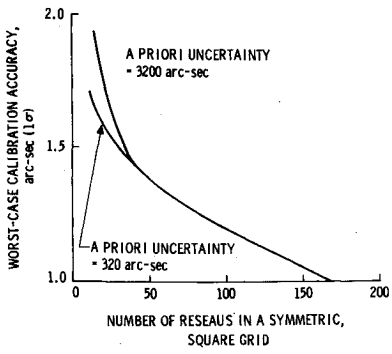

Fig. 5 Calibration accuracy of electromagnetic distortion as a function of reseaux in the grid.

The terms $\mathbf{x}_{em}$ and $\mathbf{x}_{op}$ represent electromagnetic and optical distortions, respectively. The electromagnetic distortion, containing a null-offset, symmetric radial distortion Δ_{sr}, symmetric tangential distortion Δ_{st}, and common and nonorthogonal rotations, is given by $\mathbf{x}_{em} = \mathbf{x}_0 + A\mathbf{x}_a + B\mathbf{x}$ where

$$A = \begin{bmatrix} 0 & -(\xi_1 + \xi_2) \\ \xi_1 & 0 \end{bmatrix}$$
$$B = \begin{bmatrix} \Delta_{sr} & -\Delta_{st} \\ \Delta_{st} & \Delta_{sr} \end{bmatrix} \quad (4)$$

$$\Delta_{sr} = \sum_{i=1}^{M_1} \alpha_{2i-2} r^{2i-2} \quad (5)$$

$$\Delta_{st} = \sum_{i=1}^{M_2} \alpha_{2i-1} r^{2i-1} \quad (6)$$

α_i are electromagnetic distortion coefficients; r is the distance between image and electromagnetic null point in x_1x_2

$$r = (\mathbf{x}^T\mathbf{x})^{1/2}$$
$$\mathbf{x} = \mathbf{x}_i - \mathbf{x}_n$$

$\mathbf{x}$ is the absolute location of image in X_1X_2; $\mathbf{x}_o$ is the offset between arbitrary and absolute coordinate system origins; $\mathbf{x}_n$ is the offset of electromagnetic null from origin of X_1X_2.

The optical distortion, containing a null offset, a symmetric radial distortion δ_{sr}, an asymmetric radial and tangential distortion $\boldsymbol{\delta}_p$, and a lens misalignment distortion $\boldsymbol{\delta}_m$, is given by

$$\mathbf{x}_{op} = \delta_{sr}\mathbf{x} + \boldsymbol{\delta}_p + \boldsymbol{\delta}_m \quad (7)$$

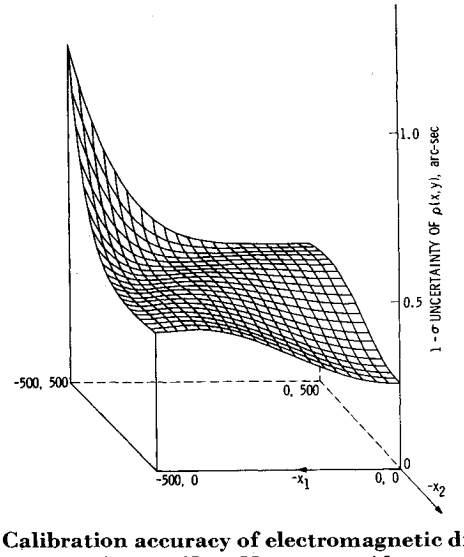

Fig. 6 Calibration accuracy of electromagnetic distortion using an 11 × 11 reseau grid.

where

$$\delta_{sr} = \sum_{i=1}^{M_3} \beta_{2i-2} r^{2i-2}$$

$$\boldsymbol{\delta}_p = \delta_a \operatorname{col}(-\sin\theta, \cos\theta) \quad (8)$$

$$\delta_a = \sum_{i=1}^{M_4} \beta_{2i-1} r^{2i} \quad (9)$$

$$\boldsymbol{\delta}_m = \mathbf{x}d^T\mathbf{x} + \gamma_3 H\mathbf{x} \quad (10)$$

$$d = \operatorname{col}(\gamma_1, \gamma_2)$$

$$H = \begin{bmatrix} 0 & -1 \\ 1 & 0 \end{bmatrix}$$

β_i are symmetric and asymmetric optical distortion coefficients; γ_i are lens misalignment distortion coefficients; r is the distance between image and principal point in X_1X_2;

$$r = (\mathbf{x}^T\mathbf{x})^{1/2}$$
$$\mathbf{x} = \mathbf{x}_i - \mathbf{x}_p$$

$\mathbf{x}$ is the absolute location of the image in X_1X_2; $\mathbf{x}_p$ is the offset of principal point from origin of X_1X_2; and θ is the distortion orientation.

From Eq. (1), it can be seen that the direction $\mathbf{t}$ to an object can be reconstructed using the measured image location, the instrument focal length, and the instrument-pointing direction. The accuracy of this reconstructed direction is determined by the accuracy with which the parameter set $\mathbf{q} = \text{col}\ (f, \epsilon_1, \epsilon_2, \epsilon_3, \mathbf{x}_0, \mathbf{x}_n, \mathbf{x}_p, \alpha_0, \alpha_1, \alpha_2, \ldots, \xi_1, \xi_2, \beta_0, \beta_1, \beta_2, \ldots, \gamma_1, \gamma_2, \gamma_3, \theta)$ is known at the time of the measurement. Therefore, the object of an instrument geometric calibration is to determine $\mathbf{q}$ from inflight data to an accuracy such that the uncertainty in $\mathbf{t}$ is less than 5 arc-sec (1σ).

A reseau grid etched onto the target raster is commonly used for calibrating the electromagnetic distortion. The absolute locations of each reseau in the grid would be measured precisely on Earth. Differences between inflight measurements of reseau locations from their absolute locations would be used in an estimation process to determine the coefficients of electromagnetic distortion (Eq. 2).

Clusters of stars would be imaged to calibrate the optical parameters. The instrument would be moved by exercising the gimbaled platform to image the star cluster at various locations on the target raster. Since calibration of optical distortion is in reference to cluster of stars, the process also involves the calibration of instrument-pointing direction.

When the gimbaled platform is not commanded to move, the errors between the actual and measured instrument orientation are characterized by

$$\epsilon^T = \left(\sum_{i=1}^{3} e_{1i}, \quad \sum_{i=1}^{3} e_{2i}, \quad \sum_{i=1}^{3} e_{3i} \right) \quad (11)$$

where e_{j1} are constant biases that are perfectly correlated between picture frames; e_{j2} are slowly varying biases that are

Table 1 Electromagnetic parameter uncertainty—1σ

Parameter	Unit	Standard deviation	
		A priori	A posteriori
$\mathbf{x}_0$	arc-sec	1000	1.3×10^{1}
$\mathbf{x}_n$	arc-sec	1000	9.7
α_0	arc-sec/pixel	2.0	5.0×10^{-3}
α_1	arc-sec/pixel^2	2.8×10^{-3}	7.3×10^{-5}
α_2	arc-sec/pixel^3	4.0×10^{-6}	3.7×10^{-8}
α_3	arc-sec/pixel^4	5.6×10^{-9}	2.7×10^{-11}
α_4	arc-sec/pixel^5	8.0×10^{-12}	6.3×10^{-14}
α_5	arc-sec/pixel^6	1.1×10^{-14}	2.5×10^{-16}
ξ_1	arc-sec/pixel	2.0×10^{-1}	2.0×10^{-3}
ξ_2	arc-sec/pixel	2.0×10^{-1}	1.7×10^{-2}

correlated but not perfectly correlated between picture frames; e_{j3} are random biases that are uncorrelated between picture frames; and $j = 1,2,3$.

These instrument pointing errors can be modeled by the following linear stochastic differential equation:

$$\dot{e}_{ij}(t) = -e_{ij}(t)/T_{ij} + \xi_{ij} \tag{12}$$

where ξ_{ij} is a Gaussian white noise process with zero-mean and variance σ_{ij}; T_{ij} is a correlation time; and $i,j = 1,2,3$.

Constant and random bias noise processes are conveniently represented by the limit processes of $T_{i1} \to +\infty$ and $T_{i3} \to +0$, respectively.

Calibration of Electromagnetic Distortion

A calibration philosophy was chosen such that sufficient reseau data would be available in each data frame to allow the calibration of electromagnetic distortion in that data frame to arc-sec accuracy independent of data from any other data frame. This philosophy was chosen because of the time varying nature of electromagnetic distortion from frame to frame due to deflection field interferences from other instruments and image charges on the vidicon tube. No attempt was made to determine possible accuracy improvements when electromagnetic distortion information from one data frame is used in the determination of distortion in another data frame.

A minimum variance sequential estimation process[7] was used in performing a covariance analysis of the expected accuracy of calibrating electromagnetic distortion using a reseau grid. A symmetric reseau grid was investigated where for each reseau at location (x_{a_1},x_{a_2}), reseaux were also located at $(x_{a_1},-x_{a_2})$, $(-x_{a_1},x_{a_2})$, and $(-x_{a_1},-x_{a_2})$. A reseau was also located at the center of the target raster (0,0). The reseaux were evenly spaced and spanned the target raster.

The accuracy of calibrating the parameter set $\mathbf{q}_{em} = \text{col}(\mathbf{x}_n, \mathbf{x}_1,\xi_1,\xi_2,\alpha_0,\alpha_1,\alpha_2,\alpha_3,\ldots)$ was determined as a function of the number of reseaux in the grid and the a priori uncertainty of $\mathbf{q}_{em}$. The location uncertainty of a point $\mathbf{x}$ on the target raster is described by the (2×2) covariance matrix

$$\Gamma_{\mathbf{x}} = [\partial \mathbf{x}_m/\partial \mathbf{q}_{em}]\Gamma_{\mathbf{q}_{em}}[\partial \mathbf{x}_m/\partial \mathbf{q}_{em}]^T \tag{13}$$

where $\Gamma_{\mathbf{q}_{em}}$ is the covariance matrix of $\mathbf{q}_{em}$ generated by the estimation process after processing the measured locations of the reseaux. The calibration accuracy of a point on the target raster is defined by

$$\rho(\mathbf{x}) = [\text{Trace}\Gamma_{\mathbf{x}}]^{1/2} \tag{14}$$

The a priori uncertainty of $\mathbf{q}_{em}$ used in this investigation is listed in Table 1. These values chosen were such that each parameter caused a 1000 arc-sec uncertainty at the corners of the target raster, except ξ_1 and ξ_2 which caused 100 arc-sec uncertainties at the corners. Experience with the narrow-angle Mariner Mars TV cameras, where the total distortion from all sources was less than 100 arc-sec, indicates that the uncertainties used in this investigation are conservative. Also, coefficients through α_3 are generally sufficient to fit the Mariner TV distortions. A contour which shows the a priori uncertainty mapped over a quadrant of the target raster is shown in Fig. 4.

Table 2 Optical parameter uncertainty—1σ

Parameter	Unit	Standard deviation	
		A priori	A posteriori
f	mm	9.5×10^{-1}	9.2×10^{-1}
e_{j1}	mrad	3.0	1.2
e_{j2}	mrad	1.0×10^{-1}	4.2×10^{-2}
e_{j3}	mrad	3.0×10^{-1}	2.2×10^{-1}
$\mathbf{x}_p$	arc-sec	1.0×10^{2}	5.3×10^{1}
θ	rad	1.0	2.0×10^{-1}
γ_1	arc-sec/pixel^2	4.0×10^{-4}	3.0×10^{-6}
γ_2	arc-sec/pixel^2	4.0×10^{-4}	3.4×10^{-6}
γ_3	arc-sec/pixel	2.0×10^{-1}	6.6×10^{-4}
β_0	arc-sec/pixel	2.0×10^{-1}	4.8×10^{-2}
β_1	arc-sec/pixel^2	2.0×10^{-4}	2.4×10^{-6}
β_2	arc-sec/pixel^3	4.0×10^{-7}	6.1×10^{-9}
β_3	arc-sec/pixel^4	4.0×10^{-10}	2.3×10^{-10}

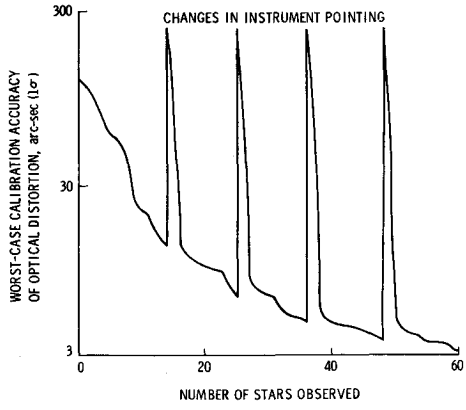

Fig. 7 Calibration of optical distortion.

Figure 5 shows the worst-case calibration accuracy, $\rho(500, 500)$, as a function of the number of reseaux in the grid. Also shown in the figure is the worst-case calibration accuracy with the a priori uncertainty reduced an order of magnitude. The figure shows that the calibration accuracy becomes essentially independent of a priori uncertainty when more than 50 reseaux are in the grid. Figure 6 shows the expected calibrated accuracy over a quadrant of the target raster when data from an 11×11 reseau grid are used. Table 1 also lists the a posteriori uncertainty of $\mathbf{q}_{em}$ for an 11×11 grid.

The conclusions derived from the investigation of electromagnetic distortion were: 1) with a symmetric reseau grid and the electromagnetic null point at the center of the reseau grid, calibration accuracy is symmetric about the null point; 2) the calibration accuracy within 500 pixels of the electromagnetic null point is better than 0.5 arc-sec (1σ) when using an 11×11 reseau grid; 3) an 11×11 reseau grid enables a worst-case calibration accuracy of 1.2 arc-sec (1σ) for each frame of data, essentially independent of a priori uncertainty and data from any other data frame.

Calibration of the Optical System

Normally, the optical distortion of a narrow angle camera is less than the scan resolution of its vidicon and exhibits long term stability (repeatability). The major uncertainty associated with the optics is in the pointing direction of the optical axis at shutter time. Imaging star clusters whose directions are essentially perfectly known is an ideal source data for calibrating the optical system. Following the conservative philosophy associated with electromagnetic distortion calibration, it will be assumed that the optical system will be calibrated during each planet approach and that the

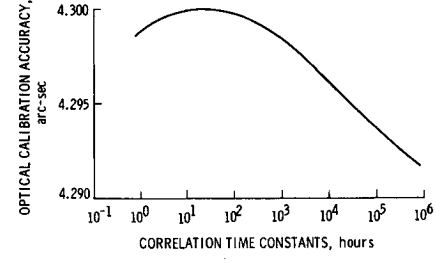

Fig. 8 Calibration accuracy as a function of correlation time constants using 50 star images.

optical distortion is repeatable during a 20 to 30 day navigation measurement period.

A cluster of stars was selected in the neighborhood of "Coma Berenices" to investigate the calibration of the optical parameters and instrument pointing direction. Stars brighter than seventh visual magnitude were assumed to be observable by using long exposure times (5 sec). The number of stars observed in one data frame would range from ten to fourteen. The instrument, mounted on a gimbaled platform would be moved several times (at 15 min intervals) to attain calibration information throughout the instrument FOV.

The a priori parameter uncertainties used in the investigation of optical distortion are listed in Table 2. The uncertainty values of optical distortion were chosen such that each parameter contributed a 100 arc-sec uncertainty at the edge of the target raster. The uncertainty values for the pointing error parameters were based on present accuracies associated with the Mariner spacecraft. Experience with Mariner narrow-angle science TV cameras, which have negligible optical distortion, indicates that the uncertainty values used in the investigation were conservative.

Figure 7 illustrates the expected worst-case calibrated accuracy of the optical system as a function of star images. The significant degradations in the figure resulted from movement uncertainty of the gimbaled platform. Calibration accuracy is quickly restored by processing a few stars in a new data frame. To accomplish 4.3 arc-sec calibration accuracy for optical distortions and instrument pointing direction uncertainty, observations of approximately 50 star images were needed. Table 2 lists the a posteriori uncertainty of the optical system parameters when 50 star images were studied.

A parametric study determining the effect of the bias correlation times (Fig. 8) showed that calibrated accuracy was very insensitive to correlation times. From these results, it is concluded that: 1) observations of approximately 50 stars facilitates the calibration accuracy of optical distortions to better than 5 arc-sec (1σ); 2) changes in correlation times of sequentially correlated biases representing instrument pointing direction errors have little effect on the calibrated accuracy; and 3) many stars (>10) can be imaged simultaneously within the instrument FOV with the capability of detecting stars brighter than 7th magnitude.

Conclusions

The worst-case uncertainty in reconstructed object direction would be less than 5 arc-sec (1σ) when using an 11×11 reseau grid and star clusters to perform an inflight calibration. The uncertainty in reconstructed object direction of an image within 500 pixels from the center of the target raster would be less than 2.5 arc-sec (1σ). Approximately 50 star images are needed to obtain this level of accuracy.

A significant developmental effort is still required before this type of instrument is flight worthy. The 9 to 12 yr outer planet missions require long life time instruments. Dynamic range and sensitivity is a problem area due to the brightness of the satellites as compared to the dim reference stars. Also, since optical measurements are only an element of the navigation system, additional effort is needed in the areas of Earth-based radio tracking measurements and planetary and natural satellite ephemeris development to yield a highly accurate, reliable and complementary system.

References

[1] Long, J. E., "Missions to the Outer Planets," *Aeronautics and Astronautics*, Vol. 7, No. 6, June 1969, pp. 32–47.

[2] Breckenridge, W. G. and Duxbury, T. C., "Defining a Spacecraft-Based Navigation Measurement System," *Aeronautics and Astronautics*, Vol. 8, No. 6, May 1970, pp. 44–49.

[3] Duxbury, T. C., "A Spacecraft-Based Navigation Instrument for Outer Planet Missions," *Journal of Spacecraft and Rockets*, Vol. 7, No. 8, Aug. 1970, pp. 928–933.

[4] Ball, J. E. and Duxbury, T. C., "Navigating the Grand Tours," *Aeronautics and Astronautics*, Vol. 8, No. 9, Sept. 1970, pp. 73–76.

[5] Wong, K. W., "Geometric Calibration of Television Systems," paper presented at the 11th International Congress of Photogrammetry, International Society of Photogrammetry, Lusanne, Switzerland, July 1968.

[6] *Manual of Photogrammetry*, edited by M. M. Thompson, American Society of Photogrammetry, Falls Church, Va., 1968, pp. 461–490.

[7] Griffin, R. E. and Sage, A. P., "Sensitivity Analysis of Discrete Filtering and Smoothing Algorithms," *AIAA Journal*, Vol. 7, No. 10, Oct. 1969, pp. 1890–1897.